Processing and Microstructure of Alumina-Based Composites

M. Mujahid, M.I. Qureshi, M. Islam, and A.A. Khan

(Submitted 13 November 1998; in revised form 26 January 1999)

A study of powder structure and its effect on the sintering tendency of certain alumina-based ceramic systems, that is, Al_2O_3-SiO_2 and Al_2O_3-ZrO_2, was carried out to improve their mechanical strength and fracture toughness. The compacting behavior and the sintering characteristics were optimized through control of various parameters such as composition, compaction pressure, sintering temperature, and time. Best densification was obtained for mixtures prepared using very fine and deagglomerated alumina powders.

Keywords alumina, alumina silica, alumina zirconia, composites, powders

1. Introduction

In recent times, advanced ceramics have been developed at a remarkable pace due to continued development in the field of powder processing (Ref 1-5). The major problem faced by ceramic materials is their inherent brittleness, and various toughening techniques have been employed to improve the fracture toughness of engineering ceramics. Some of these techniques include control of the sintered density by proper sintering procedures, use of finer powders, and control of size and concentration of pores and microcracks in sintered products (Ref 6-11). There has also been an attempt to optimize the processing route for SiC particle reinforced oxynitride glass aimed at improving hardness and fracture toughness (Ref 12). Another popular method of combating low fracture toughness of the ceramics involves introduction of various synthetic crack-retarding phases leading to toughening via phase transformation or through microcracking. Marked increase in the bend strength and fracture toughness was observed when the alumina matrix was reinforced through metastable, tetragonal zirconia particles of an average size of 0.7 μm. In such cases, the increase in mechanical properties was attributed to transformation toughening through partially stabilized zirconia particles (Ref 7-11).

In addition to general characteristics—low density, high chemical inertness, high hardness, and high temperature stability—the alumina-based ceramics offer the advantage of ease of processing. Sintered Al_2O_3-ZrO_2 and TiB_2-TiC-SiC ceramic-based composites have been successfully prepared through colloidal processing using proper deflocculants and adjustment of pH. A recent study has indicated the significant contribution of stabilized zirconia toward transformation and microcrack toughening in zirconia toughened alumina (ZTA) produced from nanocrystalline precursors (Ref 13). The hot pressing process, although expensive, involves simultaneous pressing and sintering and has been used for the production of ceramics and ceramic-based composites. Despite certain technological difficulties associated with the particulate injection molding (PIM) process, it is poised for wider acceptance and rapid growth as far as its usage in the production of advanced ceramics and composites (Ref 14).

Considerable research has been conducted over the past 15 years to study the possibilities of toughening or strengthening of ceramics by forming composites with second phase particles within a ceramic matrix. Particularly in the case of alumina-based composites, metal as well as ceramic second phase particles were found to impart an increase in mechanical and thermal shock resistance (Ref 6-10). This type of particulate composite can be prepared using powder processing technology developed for traditional ceramics, that is, mixing of the constituents in powder form followed by slip casting or compaction and using the appropriate sintering cycle. Alumina slips can be prepared in an aqueous as well as an organic medium (Ref 15).

In each case, the processing and composition of powders prior to sintering remains the key factor to obtaining desired properties. Metallic powders are difficult to manipulate due to their increased reactivity, especially in a finely divided state. Often inert atmospheres are required to sinter ceramic-metal powder mixtures. Conversely, use of a stable oxide for a second phase provides the facility to process and sinter under a normal atmosphere. Moreover, oxide ceramic slurries can usually be prepared in an aqueous medium with a controlled pH to obtain complete dispersion of powders.

In this article some preliminary results are presented that highlight the effect of concentration of silica/zirconia and the size and morphology of alumina particles on the sinterability of Al_2O_3-SiO_2 and Al_2O_3-ZrO_2 systems. The processing route employed for this study was similar to the route used for conventional ceramics, that is, mixing of the two powders in water with a suitable dispersing agent and binder, drying of the slurry, milling, and compaction to form a green pellet followed by sintering under ambient atmosphere.

2. Experimental Materials and Methods

Particle characterization (size and shape) was carried out by scanning electron microscopy (SEM) for alumina, silica, and

M. Mujahid, M.I. Qureshi, M. Islam, and **A.A. Khan,** Faculty of Metallurgy and Materials Engineering, GIK Institute of Engineering Sciences & Technology, Topi, NWFP-23460, Pakistan.

zirconia powders using a Philips XL30 scanning electron microscope (Philips Electron Optics, Eindhoven, Netherlands). The samples for this procedure were prepared by mixing a small amount of powder in a very dilute aqueous sodium phosphate solution. A tiny drop out of this solution was then transferred onto the SEM specimen stub and dried for examination under the microscope.

Table 1 provides a list of ceramic mixture compositions studied in the present work. In order to prepare composite mixtures, the constituent powders were weighed in various proportions and mixed thoroughly by making an aqueous suspension. A small amount of sodium phosphate was again added to this suspension to act as a dispersant. Using a magnetic hot plate, the suspension was simultaneously heated and stirred until dried. The dried mass was then mixed with a plasticizer (polyvinyl alcohol) and ground to further ensure the uniform distribution of constituent powders. The mixture was then cold pressed in a steel die (with 13.8 mm internal diameter) using a hydraulic press (Fig. 1) at a maximum applied pressure of 200 MPa.

Sintering of the cold-pressed green pellets was conducted in a programmable Carbolite (Carbolite Furnaces Ltd., Sheffield, UK) furnace at a maximum temperature of 1500 °C using a predetermined heating and cooling cycle (Fig. 2). The density of the sintered pellets was determined and tabulated in terms of the percentage densification given in Table 2 (Ref 16).

3. Results and Discussion

After sintering, the pallets were sectioned and polished for examination by SEM. As shown in Fig. 3(a) and (b), two types of alumina powders were used in this work: one powder with

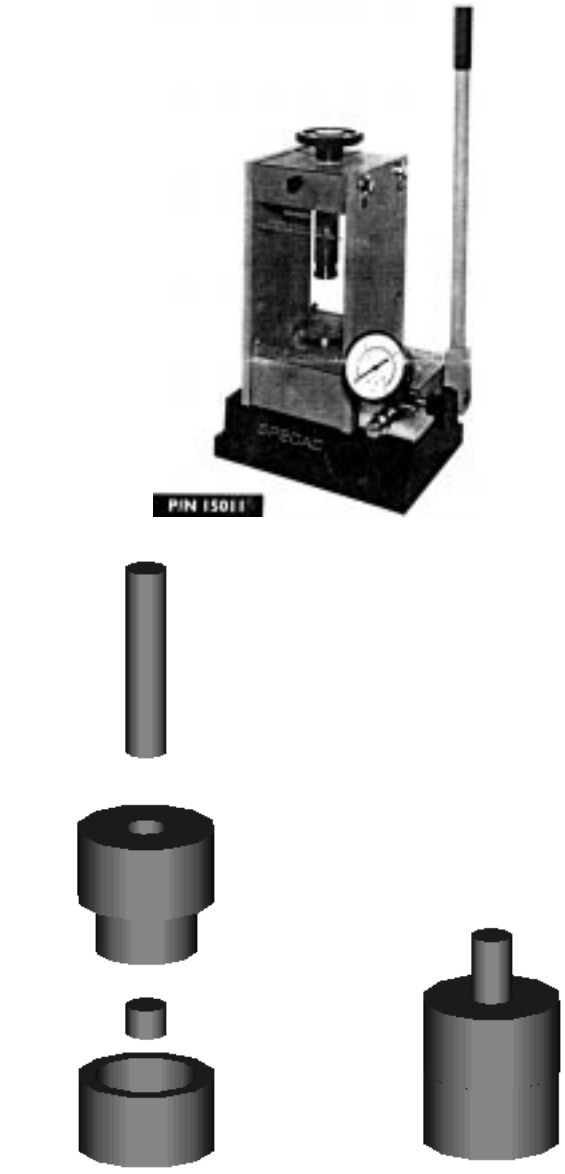

Fig. 1 Schematic diagram of the hydraulic press and dies used for compacting of powders

Table 1 Composition and theoretical density of pure as well as mixed composites

Sample No.	Sample designation	Composition, wt%	Theoretical density, g/cm^3
1	CA	Coarse Al_2O_3 (pure)	3.87
2	CAS1	90 Coarse Al_2O_3-10 SiO_2	3.75
3	CAS3	70 Coarse Al_2O_3-30 SiO_2	3.50
4	FA	Fine Al_2O_3 (pure)	3.87
5	FAS1	90 Fine Al_2O_3-10 SiO_2	3.75
6	FAS3	70 Fine Al_2O_3-30 SiO_2	3.50
7	FAZ1	90 Fine Al_2O_3-10 ZrO_2	4.04

Table 2 Sintered density and densification for different compositions

Sample No.	Sample name	Sintered density, g/cm^3	Densification, %
1	CA	2.80	72.35
2	CAS1	2.26	60.25
3	CAS3	2.22	63.48
4	FA	3.75	96.89
5	FAS1	3.47	92.74
6	FAS3	2.46	70.14
7	FAZ1	3.63	90.03

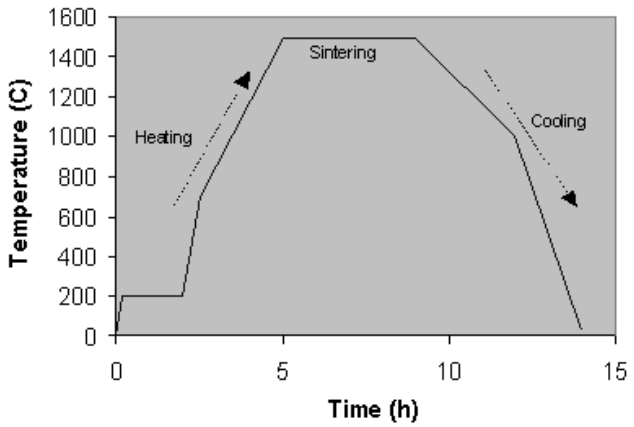

Fig. 2 Typical thermal cycle used for sintering of cold pressed green pellets

particles in hard agglomerated form (C-alumina) and the other powder a fine grade (F-alumina). The agglomerate size range in C-alumina was found to be between 7 and 78 μm, with approximately 70% of the particles lying in the range of 10 to 50 μm. The particles within the clusters ranged in size from 3 to 7 μm. The F-alumina, however, had a submicronic size range of 0.1 to 0.5 μm (Fig. 3b). The silica powder used in this study (Fig. 4a) was sieved out from a very coarse silica powder, and particles less than 45 μm were separated by using fine sieves. As can be seen in Fig. 4(a), more than 80% of the particles are in the 5 to 45 μm size range. Zirconia powder, as shown in Fig. 4(b), was also composed of agglomerates (2 to 50 μm). The zirconia particles in the agglomerates, however, were of submicronic size (approximately 0.5 μm).

Table 1 shows the sintering behavior of pure alumina, as well as other alumina-based composites. It can be observed that C-alumina, even in pure state, attains a maximum densification of only 72%, whereas F-alumina can be densified under the same sintering conditions to almost 96% of its theoretical density. The low density achieved in sintered C-alumina is believed to be due to the hard agglomerates of alumina powder that did not break during cold compaction. The particle (i.e., agglomerate) contact as manifested by neck formation is very limited. Moreover, it indicates that it has little effect on the existing porosity size (at least at the prevailing sintering temperatures). Conversely, the necking occurs at the fine particle level in F-alumina samples resulting in a substantial elimination of porosity.

In the case of $90Al_2O_3$-$10SiO_2$ ceramic mixtures, a better densification (92%) was obtained for compositions prepared using F-alumina as compared to those prepared with C-alumina (densification ~60%). The lower sintered density in mixtures containing C-alumina can again be attributed to the presence of hard agglomerates.

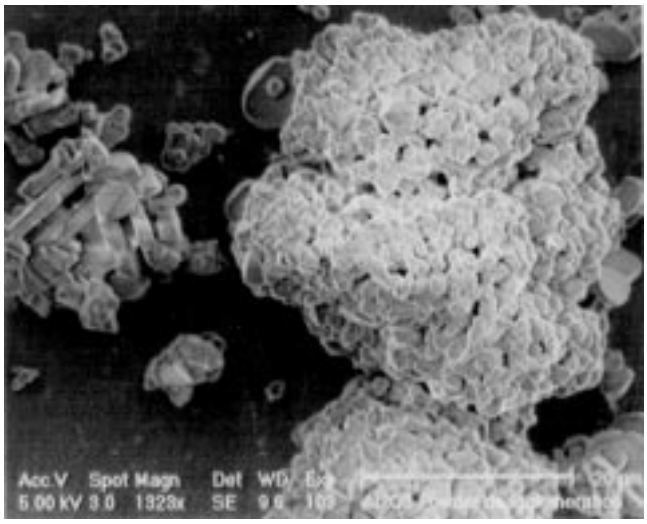

(a)

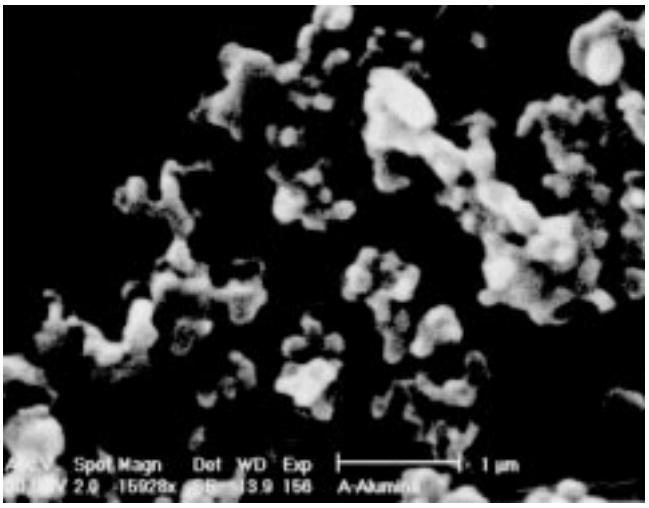

(b)

Fig. 3 Scanning electron micrographs of alumina powders. (a) C-alumina. (b) F-alumina

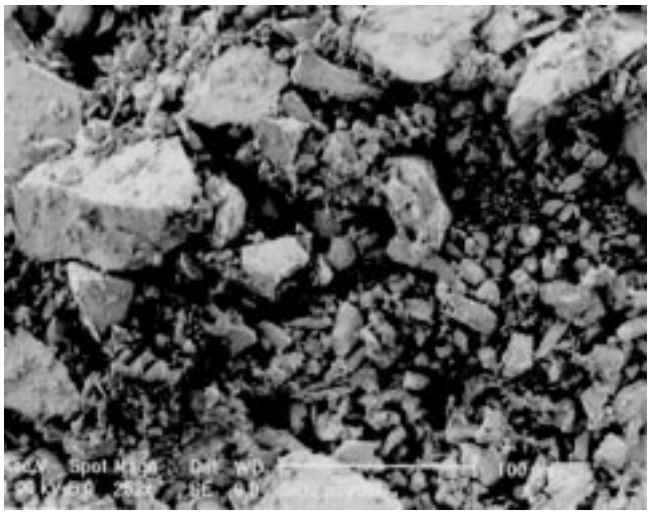

(a)

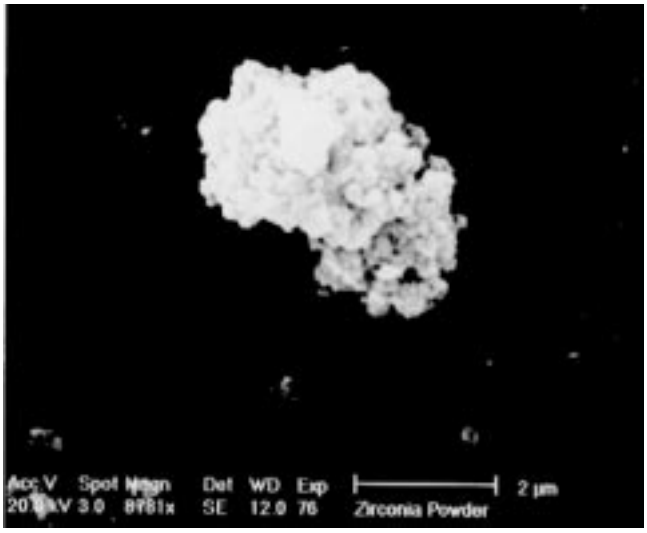

(b)

Fig. 4 Scanning electron micrographs showing (a) wide particle size range of silica powder and (b) soft agglomerates of zirconia powder

The scanning electron micrographs shown in Fig. 5 illustrate the sintered microstructures of pure F-alumina (FA), 90%F-alumina-10%SiO_2 (FAS1), and 70%F-alumina-3%SiO_2 (FAS3) samples. With the exception of sample FAS3 (densification ~70%), all the composites attained a sintered densification of greater than 90%. The composites made from C-alumina (samples CAS1 and CAS3) could only achieve a maximum densification of approximately 64% after sintering. Figure 6 shows a SEM image of composite sample CAS3 where large size porosity can be observed between the partially sintered areas. These large pores may have been left behind in the cold compaction process due to either bridging of coarse silica particles or unbreakable hard agglomerates of alumina powder. Thus, a higher amount of porosity would be expected even after the sintering of C-alumina composites as compared to F-alumina composites. One interesting point to be noted in Fig. 6 is the formation of neck, which occurs between the large agglomerates. The size of the neck is obviously comparable to the size of the agglomerates, thus requiring a massive material transfer through diffusion in solid state and evaporation con-

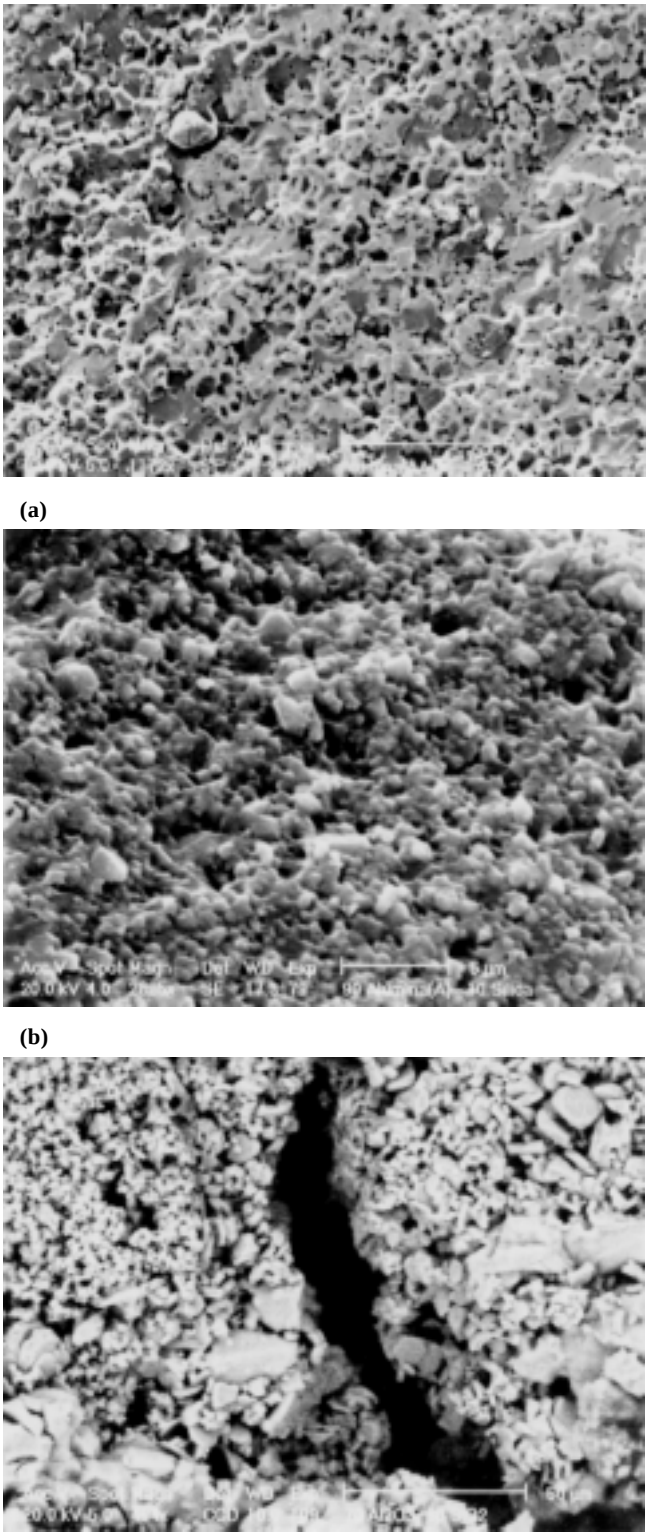

(a)

(b)

(c)

Fig. 5 Scanning electron micrographs of sintered products. (a) F-alumina with 96% densification. (b) FAS1 composite with 92% densification. (c) FAS3 composite with 70% densification

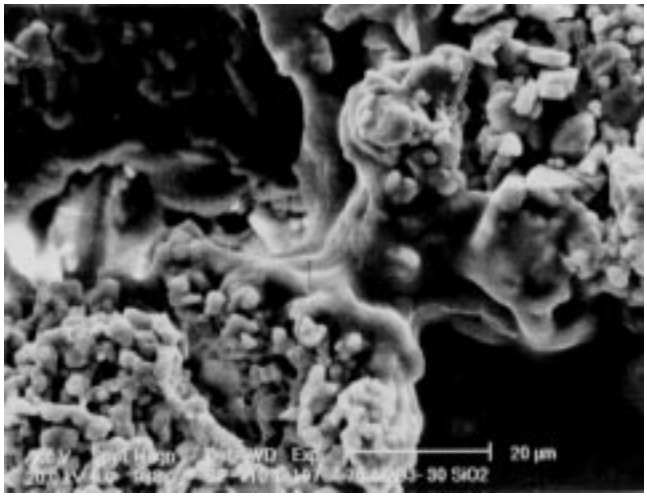

Fig. 6 Scanning electron micrographs of composite (CAS3), made with C-alumina and 30% silica, showing large size pores. Necking can also be observed.

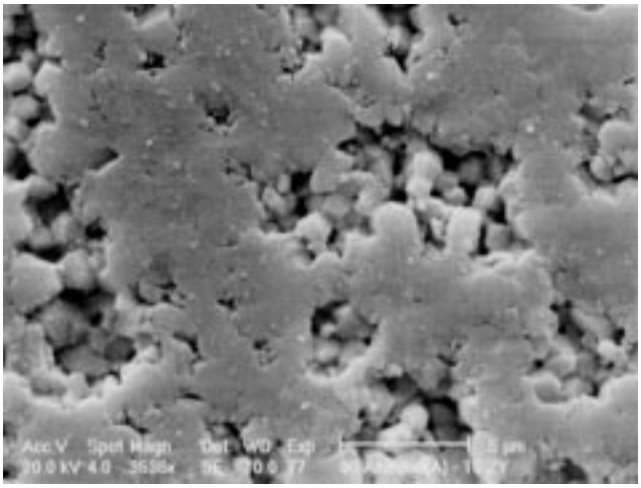

Fig. 7 Scanning electron micrograph of sintered 90% alumina-10% zirconia composite

densation in gaseous state to accomplish the task of filling this neck. This can be difficult at the prevailing sintering temperatures, resulting in reduced densification.

The composites produced using 10% zirconia in F-alumina matrix have shown a densification of approximately 90%. The SEM image in Fig. 7 reveals the microstructure of such a composite where a smaller amount of fine porosity is seen in a largely sintered matrix. The higher density achieved in Al_2O_3-ZrO_2 composite samples can be attributed to the presence of fine alumina powder particles and soft agglomerates of zirconia powder. This condition can help achieve higher densities in both cold compaction and subsequent sintering processes through local neck formation between fine submicronic particles.

4. Conclusions

The following conclusions can be drawn:

- The sintering behavior depends primarily on the nature and size range of powder particles. Hard agglomerates of C-alumina powder were difficult to break during cold compaction and subsequently gave low densification upon sintering.
- A critical limit exists on the second phase (silica powder) reinforcement volume that can be accepted by the alumina matrix in order to achieve a densification of >90%. The exact value of this limit remains to be verified, but it can be stated that if large size second phase particles are present, they hinder the die cold pressing process and finally reduce the sintered density. In this study, the authors observed that an addition of 30% SiO_2 particles drastically reduced the sintered density of the composite to 70% of its theoretical density.

Acknowledgment

The authors would like to acknowledge the GIK Institute of Engineering Sciences and Technology for the use of laboratory facilities.

References

1. V.A. Tracey, *Powder Metall.*, Vol 35, 1992, p 93
2. A. Bose, H.R. Couque, and J. Lankford, Jr., *Int. J. Powder Metall.*, Vol 24, 1992, p 383
3. R.K. Dube, *Powder Metall.*, Vol 33, 1990, p 119
4. J. Dickson, *Modern Developments in Powder Metallurgy*, Vol 18, Metal Powder Industries Federation, Princeton, NJ, 1988, p 775
5. R.L. Martin and R.J. Lederich, *Advances in Powder Metallurgy*, Vol 6, Metal Powder Industries Federation, Princeton, NJ, 1991, p 361
6. C.S Mogan, A.J. Moorehead, and R.J. Loaf, *Amer. Ceram. Soc. Bull.*, Vol 61 (No. 9), 1982, p 974
7. W.H. Tuan and R.J. Brook, *J. Eur. Ceram. Soc.*, Vol 6 (No. l), 1990, p 31
8. P.A. Trusty and J.A. Yeomans, *J. Eur. Ceram. Soc.*, Vol 17 (No. 4), 1997, p 495
9. J.L. Besson, P. Boch, and T. Chartier, Materials Science Monographs, *Tech. Ceram.*, Vol 38, 1987, p 633
10. H.M. Jang, S.M. Cho, and K.T. Kim, *J. Mater. Sci.*, Vol 32 (No. 2), 1997, p 503
11. S. Jiao, M.L. Jenkins, and R.W. Davidge, *Acta Metall.*, Vol 45 (No. 1), 1997, p 149
12. T. Chartier and T. Rouxel, *J. Eur. Ceram. Soc.*, Vol 17 (No. 2-3), 1997, p 299
13. J. Friem and J. McKittrick, *J. Am. Cer. Soc.*, Vol 81 (No. 7), 1998, p 1773
14. T.L. Wong, R.K.Y. Li, and C.M.L. Wu, *J. Mat. Proc. Technol.*, Vol 63, 1997, p 399
15. S. Assmann, U. Eisele, and H. Boder, *J. Eur. Ceram. Soc.*, Vol 17 (No. 2-3), 1997, p 309
16. M. Islam, Project Report, GIK Institute, Topi, Pakistan, 1997